

## Deep learning approaches to predict sea surface height above geoid in Pekalongan

Resa Septiani Pontoh<sup>a\*</sup>, Muhammad Rivaldi Saiful Raff<sup>a</sup>, Chrysentia Clarissa Clorinda<sup>a</sup>, Absalom Zakharia Ady Ena<sup>a</sup>, Mohamad Naufal Farras<sup>a</sup>, Restu Arisanti<sup>a</sup>, Toni Toharudin<sup>a</sup> and Farhat Gumelar<sup>a</sup>

<sup>a</sup>University of Padjadjaran, Indonesia

### CHRONICLE

#### Article history:

Received: November 7, 2023

Received in revised format: November 30, 2023

Accepted: January 7, 2023

Available online: January 7, 2024

#### Keywords:

Sea surface height

Neural network

Pekalongan

Forecast

Bidirectional GRU (BiGRU)

### ABSTRACT

Rising sea surface height is one of the world's vital issues in marine ecosystems because it greatly affects the ecosystems as well as the socio-economic life of the surrounding environment. Pekalongan is one area in Indonesia facing the effects of this phenomenon. This problem deserves to be explored further with complex approaches. One of them is a neural network to perform forecasting more accurately. In neural networks, the time series approach can be used with Long Short-Term Memory (LSTM) and Gated Recurrent Unit (GRU). By adding the bidirectional method to each of these two approaches, we will find the best method to use to perform the analysis. The best results were obtained by forecasting for 960 days using Vanilla BiGRU. The results can be interpreted from multiple perspectives. The forecasting results showed a fluctuating pattern as in previous periods, so it can be said that the pattern is still quite normal, which indicates that the terminal can continue to operate normally. However, the forecasting results from this study are expected to be a reference for information for the government to prevent future dangers.

© 2024 by the authors; licensee Growing Science, Canada.

## 1. Introduction

Climate change due to global warming has now become a major threat to the world, significantly impacting economic conditions, infrastructure, and even social life. The impact amongst them is the increment of sea surface height in almost all parts of the world. Sea surface height does not just mean that the water elevates, but also warms and expands the ocean. As a result, salinity also changes, thus affecting sea levels (NASA, n.d.). In the long run, this episode will have unpropitious effects, like coastal abrasion, shoreline erosion, inundation of a land area, and even drown small islands because of the higher intensity and frequency of flooding (Watson, 2001). According to the International Panel of Climate Change (IPCC), the sea level rises as high as 3.2 mm a year (Watson, 2001).

Indonesia is an archipelagic country with a water area of around 70% of the total area, making the country susceptible to water-related climate change impacts, such as sea level rise. The Indonesian region is currently facing a slow but steady SLR problem that is starting to take over its land area. SLR is the condition in which the sea level rises above a benchmark or adjacent land point. Consequently, a tide gauge measures the relative sea level (relative to the elevation of the benchmark) as opposed to the sea level measured by a satellite altimeter, which is in relation to the center of the Earth (or geoid). The National Research and Innovation Agency (BRIN) estimated last year that at least 115 of Indonesia's islands would be submerged by 2100 due to rising sea levels and land subsidence. According to a new study, 92 of Indonesia's most remote islands could submerge due to rising sea levels (Liliansa, 2023). The sinking of these islands will affect national territorial boundaries. This

\* Corresponding author.

E-mail address: [resa.septiani@unpad.ac.id](mailto:resa.septiani@unpad.ac.id) (R. S. Pontoh)

ISSN 2561-8156 (Online) - ISSN 2561-8148 (Print)

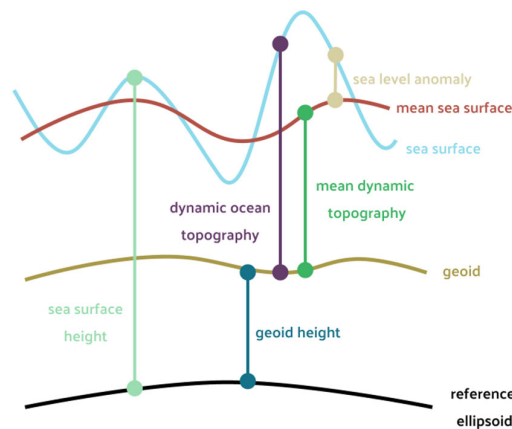
© 2024 by the authors; licensee Growing Science, Canada.

doi: 10.5267/j.ijds.2024.1.004

is essential because it can result in total territorial loss, including the loss of baselines and maritime zones calculated from them (Vinata et al., 2023).

Another problem is the form of puddles of water on the coastal plains that occur during high tides or what is known as tidal floods. Tidal floods inundated places lower than the high tide level such as coastal areas (Nashrullah et al., 2014). Currently, several areas in Indonesia have the potential to experience tidal flooding, one of which is the Pekalongan coastal area on the north coast of Java. This area has encountered a weighty rise in sea level that is higher than the Java Sea, which is approximately 5 mm per year. Meanwhile, the Java Sea is generally rising by 3.9 mm per year. If this situation continues, the Pekalongan area can sink in a few decades. Scientists have warned that if nothing is done to deal with this issue by 2036, the entire city could be submerged (Rayda, 2021). Simultaneously, climate change has also led to more extreme rainfall, gusty winds, and higher waves, in addition to sea level rise. Pekalongan often deals with flooding issues. Recurring floods have triggered the loss of assets, productive land, and infrastructure and the unsettling of public services. In addition, it requires remarkable costs for disaster preparedness, response, and recovery and those become the source of vulnerability. Disaster risk gives rise to the prospect of downgrading one's economy. Eventually, it becomes even more difficult to come up with strategies for confronting potential threats (Fitritia & Matsuyuki, 2022). Changes in rainfall patterns are also a result of climate change, as evidenced by the slight decline in Pekalongan City's annual precipitation over the past two decades. These changes will impact the frequency of flooding in the Kupang watershed's downstream region (Pekalongan coast) (Habibi et al., 2021).

Indonesia is in the equatorial region between the Indian and Pacific Oceans. The rising sea level rise, which is becoming a global issue due to climate change, is one of the marine dynamics that can undoubtedly harm islands and coastal areas in Indonesia, which are places of settlement and livelihoods. The rise in sea level is an increase in the ocean's level, culminating in a heightening of the sea surface. Sea surface height (SSH) is the elevation of the sea surface above an ellipsoid of reference. The geoid is a geopotentially constant surface, so if the ocean were at rest, the sea level would coincide. The global average of the time-mean sea surface height (i.e. mean sea level) must be zero above the geoid.



Modified from: GGOS, 2024

**Fig. 1.** Definition of various quantities related to sea surface heights.

In order to analyze the spatial and temporal evolution of sea level, Braakmann-Folgmann et al. developed a combination of Convolutional Neural Networks (CNN) and Recurrent Neural Networks (RNN) methods. They also tested their method for the northern and equatorial Pacific Ocean regions (Braakmann-Folgmann et al., 2017). Braakmann-Folgmann et al. forecasted sea levels for the next 48, 72, and 168 hours in Jakarta Bay using three deep learning techniques: recurrent neural networks (RNN), long short-term memory (LSTM), and bidirectional long short-term memory (BiLSTM). They then compared these techniques to determine which performed the best (Masri et al., 2020).

In this study, we will be concentrating on forecasting the height of the sea surface for the next period in the coastal area of Pekalongan on the north coast of Java, or furthermore near the area of the state port. LSTM, GRU, BiLSTM, and BiGRU are just some of the deep learning techniques that will be used to perform predictive analysis. The vanishing gradient issue that affects vanilla RNN is dealt with by GRU and LSTM, with LSTM generalising GRU (Toharudin et al., 2023). The features of time series can be captured by LSTM over a longer time. In artificial recurrent neural networks, GRU is seen as a kind of gate mechanism comparable to LSTM. Nevertheless, GRU demonstrates better performance with small to medium datasets. BiLSTM consists of two layers of LSTM neural networks that will be applied to the input data. BiLSTM enables a better understanding by learning future time steps bidirectionally. BiGRU is a particular form of bidirectional recurrent neural network that consists of two GRU; one takes the information in a forward direction and the other in a backward way, for greater expression and learning capacity. In the finale, the performance of all methods would be compared to decide which is the best

to use for predicting sea surface height for the next 960 days (32 months) by observing each model's metrics and how the forecasting conclusion is reached.

## 2. Materials and Methods

### 2.1 Study Area and Data Collection

The data used in this study relates to the daily sea surface height above the geoid in Pekalongan's coastal region, which is part of Indonesia's Province of Central Java and is bordered to the north by the Java Sea. It has huge capabilities in the fisheries and agriculture sectors and is also known as one of the largest fishing port towns in Southeast Asia. Additional information on the study area may be found close to the Pelabuhan Perikanan Nusantara Pekalongan, which provides services to fishing boats that operate in Indonesian waters and the Indonesian Exclusive Economic Zone (ZEE). The coordinates of the point taken are 3,908.16 m from the port.



Source: <https://earth.google.com> (accessed on 26 May 2023).

**Fig. 2.** The distance between the point coordinates of the studied area (red) and the port (yellow).

Data was collected from Copernicus, an EU programme, according to satellite Earth Observation and in situ (non-space) data. It can be accessed by the public. The time-series data used is from 1 January 1993 – 30 April 2023. Forecasting analysis was conducted using several deep-learning approaches mentioned in the earlier section.

### 2.2 Long Short-Term Memory (LSTM)

Long Short Term Memory (LSTM) is one of the developments of the Recurrent Neural Network (RNN), which consists of memory units. As was discussed before, LSTM can handle disappearing gradients and overcome exploding gradients by including memory cells with stable errors that allow errors to be replicated without vanishing gradients (Zahroh et al., 2019). RNN cannot be used for data that covers an extended time, but LSTM overcomes this limitation by including a cell state, allowing the old information to be utilized (Toharudin et al., 2023). The LSTM network can handle both short-term and long-term connection in time series.

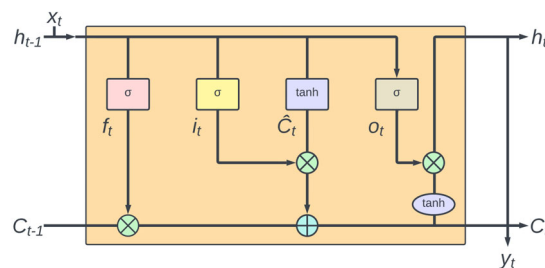


**Fig. 3.** The structure of LSTM (Modified from: Alghifari et al., 2022)

The fundamental components of the LSTM are the cell state, forget gate, input gate, and output gate, which work cooperatively to accomplish the function of the LSTM unit and control the flow of information (Jiang et al., 2019). To prevent the memory content from being disturbed by irrelevant inputs, each memory cell includes a state within it and several multiple gates that

decide whether an input's impact should affect its internal state. These multiplicative gates are referred to as input gates. The internal state of a specific neuron should then be abandoned to the forget gate, and it should be permitted to affect the cell's output or the output gate, which shields other units from disruption by currently irrelevant memory contents (Hochreiter & Schmidhuber, 1997). Sigmoid and tangent functions are activation functions that are mainly used in LSTM cells. To begin with, the predictor data are transformed into a three-dimensional format including samples, timesteps, and LSTM features (Pontoh et al., 2022).

2.3 Gated Recurrent Unit (GRU)

The GRU is an improved version of the LSTM architecture that frequently achieves similar efficiency while being faster to calculate. In the GRU cell unit, the input and forget gates are combined into one gate. The hidden state and cell state are also put together. All these modifications result in a simpler structure with just two gates: an update gate determines how much the potential activation function will be utilised to alter the cell state, and a reset gate removes previous information (Toharudin et al., 2023).

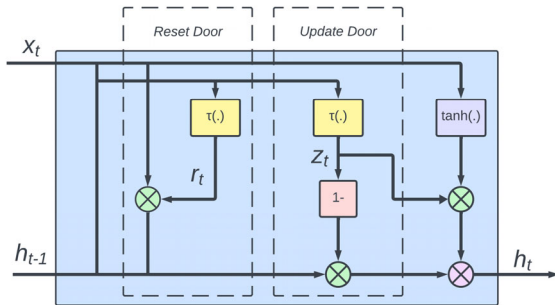


Fig. 4 A GRU cell (Modified from: Yu et al., 2023)

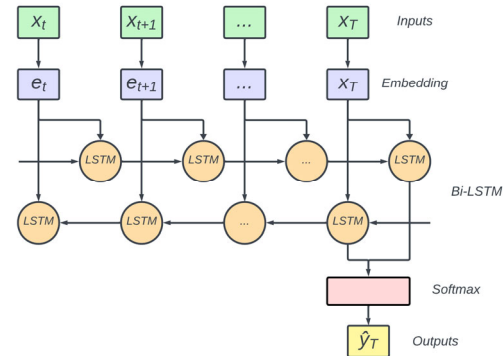


Fig. 5. The structure of the BiLSTM network (Modified: Ertugrul & Karagoz, 2018)

2.4 Bidirectional Long Short-Term Memory (BiLSTM)

Bidirectional Long Short Term Memory (BiLSTM) was first proposed by Graves and Schmidhuber in 2005 to map speech frame sequences to associated phoneme label sequences (Graves & Schmidhuber, 2005). BiLSTM comprises two LSTM networks; forward and backward. Forward direction creates a model from the prior context and a backward direction is to model the following contexts, respectively. Two opposing LSTMs are combined to form a BiLSTM. This technique can add to training while collecting time series data in two ways. BiLSTM will perform better due to more training and two-way feature extraction (Liang et al., 2021). The output at time step  $t$  is affected by both the state at time step  $t+1$  and the state at time step  $t-1$  (Masri et al., 2020). BiLSTM connects two hidden layers from both directions to the same output, while LSTM executes in a single direction only, from start to end (Isnain et al., 2020). In consequence, BiLSTM can perform better by also learning future time steps, and the BiLSTM method was able to outperform LSTM in predicting time series data (Siarnamini et al., 2019). The structure of the BiLSTM network is shown as in Fig. 5.

2.5 Bidirectional Gated Recurrent Unit (BiGRU)

This method is like BiLSTM. Two gated recurrent units (GRU) make up a bidirectional gated recurrent unit (BiGRU); one GRU forwards and the other backwards to provide more powerful expression and learning ability (Faturrohman & Rosmala, 2022).

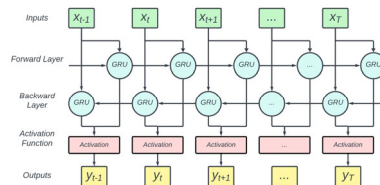


Fig. 6 The BiGRU structure (Modified from: Ju et al., 2019)

The forward direction is correlated with prior data; and the reverse direction is linked to future data, so that both input data can be used at the same time (Ju et al., 2019). This structure can effectively boost the performance of the single-direction GRU.

## 2.6 Loss Functions and Evaluation Metrics

The predicted values to the actual values could be compared to yield metrics called loss function, often referred to as the error or pseudo residual (Boehmke & Greenwell, 2019). There are many loss functions to choose from when assessing the performance of a predictive model, e.g., mean squared error (MSE) that we will use in this study. The mean squared error is the average of the squared error. MSE equals zero if a model has no error. As model error increases, its value increases. So, the objective of this function is to minimize the value (Boehmke & Greenwell, 2019).

$$MSE = \frac{1}{n} \sum_{i=1}^n (Y_i - \hat{Y}_i)^2 \quad (1)$$

Generally, we use  $R^2$  to evaluate the performance of a model. However, it is only one of the many possible ways to summarise how well a model performs on a given dataset. Many different metrics can be used for time series forecasting, including the most known ones: the mean absolute percentage error (MAPE) which will also be used in this paper.

$$MAPE = \frac{1}{n} \sum_{i=1}^n \frac{|F_i - A_i|}{A_i} \quad (2)$$

MAPE is a calculation that indicates how large a prediction's error is compared to the actual value (Khair et al., 2017). The absolute function prevents a difference between the positive and negative values (Kim & Kim, 2016). Regardless of whether individual forecasts were upscaled or inadequate, it gauges the accuracy of the predictions by displaying the average percent difference between predictions and actual data. The lower the MAPE value, the better the ability of the forecasting model. Table 1 shows the range of MAPE values that can be used as a material for measuring the ability of a forecasting model.

**Table 1**

Interpretation of MAPE values.

MAPE	Interpretation
< 10%	Very good
10% – 20%	Good
20% – 50%	Okay
> 50%	Not good

## 2.7 Methods of Analysis

This analysis was carried out by executing several processes. The method can be previewed in greater detail in Fig. 7, below with the explanation of each step provided below the image.

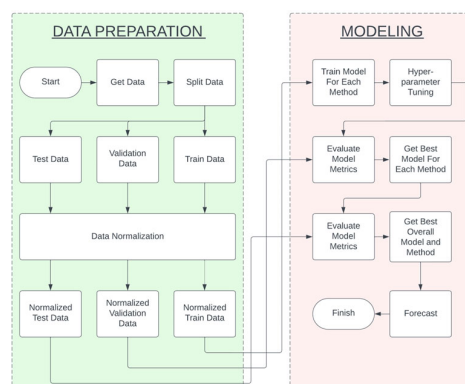


**Fig. 7.** Research Steps

The initial stage is to retrieve the data from the Copernicus Marine Services website using Miniconda and its API. The existing data is then periodized into 120-day intervals and divided into train data, validation data, and test data. Using the mean and variance parameters of the train data, each subset of data is normalized or standardized beforehand. The learning process in machine learning can be accelerated and optimized with the help of data normalization (Ambarwari et al., 2020). Training and hyperparameter tuning are then conducted on the training data using one of the twelve proposed methods. Using validation

data, the optimal hyperparameter for each method is determined based on the MAPE metric value with the smallest value. The tuned hyperparameter is the hyperparameter of the dense layer with a hyperparameter space of [4, 8], as indicated by the brackets. This dense layer is responsible for transforming vector inputs into probabilistic predictions (Shahin & Almotairi, 2021). We apply different layers and numbers of neural units to observe how the predicted values change as a result (Zhao et al., 2017). After determining the optimal hyperparameters for each method, metrics are computed using test data.

The computation determines, based on the MAPE metric for the lowest test data, the optimal technique for continued analysis. Notably, in the training model, we added two early stopping callbacks. When a training agreement is terminated, early stopping returns parameter settings at the point in time with the lowest validation set error and decreases the learning rate when the validation MAPE metric did not undergo any insignificant changes (Goodfellow et al., 2016). Additionally, the hyperparameters fixed for each method (non-tuned) are [Optimizer = RMSprop, Learning Rate = 0.01, and Epoch = 20]. The goal of optimizers is to minimize the loss function or increase the model's efficiency (Mehmood et al., 2023).

### 3. Results

The data analysis was performed using the open-source software R Studio. As previously mentioned, the methods used in this paper are LSTM, GRU, BiLSTM, and BiGRU. There are no assumptions required, so the analysis can be performed after data preprocessing. The data was periodized into periods of 120 days, with the result that the amount of data was reduced to just 93. The data was then divided into three sets, with the ratio of 6:2:2 being used for the training set, validation set, and test set.

Hyperparameter tuning is essential to controlling the complexity of the learning algorithms. The setting of these hyperparameters (layer dense) depends on the data. A small number of neurons will reduce the ability of a network to process it, whereas if the number of neurons is too large, it will cause overfitting (Panchal & Panchal, 2014). Several possible values for tuning parameters are 4, 8, and 16 because the amount of sample data tends to be tiny, so the hyperparameter would not be excessive or overparameterized. The value for the layer dense of each method used is obtained from the smallest value of the validation metrics. The result is shown in Table 2 below.

**Table 2**  
Best hyperparameter and metrics from each method

Methods	Layer Dense	Val MAPE	Time	Test MAPE
Vanilla LSTM	(8)	12.3	12.42680 secs	9.9184
2-Stacked LSTM	(16, 4)	3.02	45.70496 secs	9.9982
3-Stacked LSTM	(4, 16, 4)	9.12	20.60998 secs	8.9513
Vanilla GRU	(16)	11.0	12.70178 secs	10.9254
2-Stacked GRU	(4, 4)	8.01	22.24357 secs	9.9001
3-Stacked GRU	(4, 8, 8)	11.1	25.55397 secs	19.3601
Vanilla BiLSTM	(4)	17.3	22.15768 secs	8.5304
2-Stacked BiLSTM	(8, 16)	6.51	90.37361 secs	15.0640
3-Stacked BiLSTM	(4, 4, 4)	3.65	50.49117 secs	8.9333
Vanilla BiGRU	(4)	5.74	28.21519 secs	6.2631
2-Stacked BiGRU	(4, 4)	9.23	35.80667 secs	9.2028
3-Stacked BiGRU	(16, 8, 4)	5.05	50.92581 secs	7.8693

Table 2 shows that the minimum test MAPE is 6.2631 for Vanilla BiGRU. The result is very likely to happen because the whole dataset leans small, so the bidirectional method will perform better than the ordinary method. GRU is more likely to be selected if we compared it to LSTM since the hyperparameters are fewer. So, Vanilla BiGRU with four-layer dense is suitable to perform the analysis.

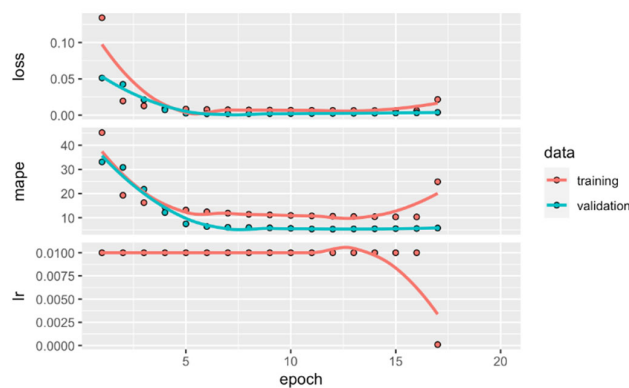


**Fig. 8** Vanilla BiGRU Epoch vs Loss, Metrics, and Learning Rate

The number of epochs that are required to give the maximum result is 17 times with a learning rate of 0.01. After the best method is chosen, forecasting analysis is performed to predict sea surface height for the next 8 periods or 960 days. In addition, the normalized data had intervals between 0 and 1, which were denormalized to provide the original results of red chili price forecasts (Bin et al., 2019).

**Table 3**  
Forecast table of sea surface height above geoid.

Time	Forecast Height
2023-07-23	0.6819638
2023-11-20	0.7271208
2024-03-19	0.6403619
2024-07-17	0.6503378
2024-11-14	0.6725675
2025-03-14	0.6147895
2025-07-12	0.5934405
2025-11-09	0.6843297

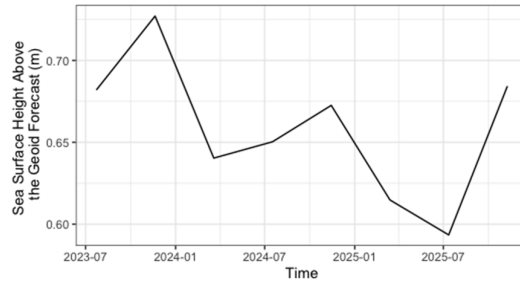


**Fig. 9** Forecast plot of sea surface height above geoid

According to the model's forecasts, the level of the sea will reach its highest point (0.727) in 20 November 2023 and its lowest point (0.593) in 12 July 2025. These results are shown in Table 3.

**4. Discussion**

The forecast outcome can be interpreted from several different perspectives. If we look thoroughly at the forecast with the actual data, which is prior to 96 months, as attached in Fig. 9, we can conclude that there is neither a significant increase nor decrease in sea surface height above the geoid. This indicates that the port can be operated as usual.

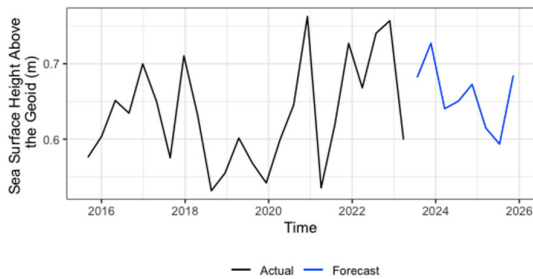


**Fig. 10.** Sea surface height above geoid actual data vs forecast

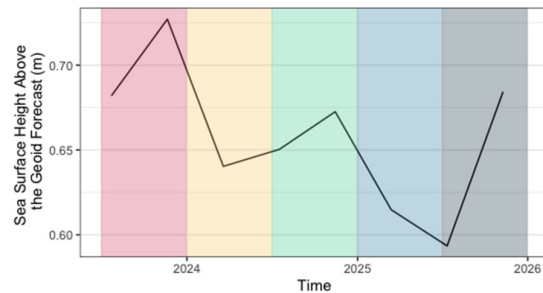


**Fig. 11.** Biannual forecast of sea surface height above geoid

Nevertheless, if we took another point of view, we would only look at the forecast. Then, we divide the graph into half-yearly phases, as shown in Fig. 11. Fig. 10 could be divided into 5 parts that are marked with five different color shades. The red shade background represented the second-half year of 2023. Yellow shade represented January–June of 2024. The green shade represented July–December of 2024, etc. A distinct pattern can be seen after we split the forecast results. In the second-half of the year, there is a constant increment of sea surface height above the geoid, whereas in the first half year is a decrease from the previous year. In 2025, sea surface height will experience a decrease even more significant than in 2024. However, in the first half year of 2026, it will mount back to the top. Therefore, the port must be aware of and prepare for this upsurge in surface height that might cause unfavorable impacts such as tidal floods, which often hit the Pekalongan area. Therefore, the government is expected to use the forecasting results in this study as a reference for anticipating the dangers that will occur.

**5. Conclusion**

Referring to the analysis that has been conducted, the best model for forecasting sea surface height above geoid with neural network is the GRU model with one layer or Vanilla GRU, with 4 nodes in the layer and MAPE for test data of 6.3%. Forecasting results for 960 days for 8 periods indicate fluctuating up and down patterns in each half-year phase. Forecasting sea level utilizing neural network is effective to implement regardless of the amount of training data.

## Funding

This research is supported by the Department of Statistics, Padjadjaran University and Rector Padjadjaran University.

## References

- Alghifari, D. R., Edi, M., & Firmansyah, L. (2022). Implementasi Bidirectional LSTM untuk Analisis Sentimen Terhadap Layanan Grab Indonesia. *Jurnal Manajemen Informatika (JAMIKA)*, 12(2), 89–99. <https://doi.org/10.34010/jamika.v12i2.7764>
- Ambarwari, A., Jafar Adrian, Q., & Herdiyeni, Y. (2020). Analysis of the Effect of Data Scaling on the Performance of the Machine Learning Algorithm for Plant Identification. *Jurnal RESTI (Rekayasa Sistem Dan Teknologi Informasi)*, 4(1), 117–122. <https://doi.org/10.29207/resti.v4i1.1517>
- Bin, Y., Yang, Y., Shen, F., Xie, N., Shen, H. T., & Li, X. (2019). Describing Video With Attention-Based Bidirectional LSTM. *IEEE Transactions on Cybernetics*, 49(7), 2631–2641. <https://doi.org/10.1109/TCYB.2018.2831447>
- Boehmke, B., & Greenwell, B. (2019). *Hands-On Machine Learning with R*. Chapman and Hall/CRC. <https://doi.org/10.1201/9780367816377>
- Braakmann-Folgmann, A., Roscher, R., Wenzel, S., Uebbing, B., & Kusche, J. (2017). *Sea Level Anomaly Prediction using Recurrent Neural Networks*.
- Ertugrul, A. M., & Karagoz, P. (2018). Movie Genre Classification from Plot Summaries Using Bidirectional LSTM. *2018 IEEE 12th International Conference on Semantic Computing (ICSC)*, 248–251. <https://doi.org/10.1109/ICSC.2018.00043>
- Faturrohman, F., & Rosmala, D. (2022, June 21). Analisis Sentimen Sosial Media dengan Metode Bidirectional Gated Recurrent Unit. *2022: Prosiding Diseminasi FTI Ganjil 2021/2022*.
- Fitritinia, I. S., & Matsuyuki, M. (2022). Role of social protection in coping strategies for floods in poor households: A case study on the impact of Program Keluarga Harapan on labor households in Indonesia. *International Journal of Disaster Risk Reduction*, 80, 103239. <https://doi.org/10.1016/j.ijdr.2022.103239>
- GGOS. (2024). *Sea Surface Heights*. Global Geodetic Observing System.
- Goodfellow, I., Bengio, Y., & Courville, A. (2016). *Deep Learning*. The MIT Press.
- Graves, A., & Schmidhuber, J. (2005). Framework phoneme classification with bidirectional LSTM networks. *Proceedings. 2005 IEEE International Joint Conference on Neural Networks, 2005.*, 2047–2052. <https://doi.org/10.1109/IJCNN.2005.1556215>
- Habibi, S., Pribadi, A., & Sitorus, J. (2021). The concept design for adaptation of climate change through integrated and sustainable flood infrastructure in the coastal area of Pekalongan, Indonesia. *Geographica Pannonica*, 25(2), 121–135. <https://doi.org/10.5937/gp25-30852>
- Hochreiter, S., & Schmidhuber, J. (1997). Long Short-Term Memory. *Neural Computation*, 9(8), 1735–1780. <https://doi.org/10.1162/neco.1997.9.8.1735>
- Isnain, A. R., Sihabuddin, A., & Suyanto, Y. (2020). Bidirectional Long Short Term Memory Method and Word2vec Extraction Approach for Hate Speech Detection. *IJCCS (Indonesian Journal of Computing and Cybernetics Systems)*, 14(2), 169. <https://doi.org/10.22146/ijccs.51743>
- Jiang, C., Chen, Y., Chen, S., Bo, Y., Li, W., Tian, W., & Guo, J. (2019). A Mixed Deep Recurrent Neural Network for MEMS Gyroscope Noise Suppressing. *Electronics*, 8(2), 181. <https://doi.org/10.3390/electronics8020181>
- Ju, Y., Zhang, M., & Zhu, H. (2019). Study on a New Deep Bidirectional GRU Network for Electrocardiogram Signals Classification. *Proceedings of the 3rd International Conference on Computer Engineering, Information Science & Application Technology (ICCIA 2019)*. <https://doi.org/10.2991/iccia-19.2019.54>
- Khair, U., Fahmi, H., Hakim, S. Al, & Rahim, R. (2017). Forecasting Error Calculation with Mean Absolute Deviation and Mean Absolute Percentage Error. *Journal of Physics: Conference Series*, 930, 012002. <https://doi.org/10.1088/1742-6596/930/1/012002>
- Kim, S., & Kim, H. (2016). A new metric of absolute percentage error for intermittent demand forecasts. *International Journal of Forecasting*, 32(3), 669–679. <https://doi.org/10.1016/j.ijforecast.2015.12.003>
- Liang, S., Wang, D., Wu, J., Wang, R., & Wang, R. (2021). Method of Bidirectional LSTM Modelling for the Atmospheric Temperature. *Intelligent Automation & Soft Computing*, 29(3), 701–714. <https://doi.org/10.32604/iasc.2021.020010>
- Liliansa, D. (2023, January 19). Sea level rise may threaten Indonesia's status as an archipelagic country. *The Conversation*.
- Masri, F., Saepudin, D., & Adytia, D. (2020). Forecasting of Sea Level Time Series using Deep Learning RNN, LSTM, and BiLSTM, Case Study in Jakarta Bay, Indonesia. *E-Proceeding of Engineering*, 8544–8551.
- Mehmood, F., Ahmad, S., & Whangbo, T. K. (2023). An Efficient Optimization Technique for Training Deep Neural Networks. *Mathematics*, 11(6), 1360. <https://doi.org/10.3390/math11061360>
- NASA. (n.d.). *Understanding Sea Level*. NASA Sea Level Change Portal. Retrieved July 10, 2023, from <https://sealevel.nasa.gov/understanding-sea-level/overview>
- Nashrullah, S., Aprijanto, -, Pasaribu, J. M., Hazarika, M. K., & Samarakoon, L. (2014). STUDY ON FLOOD INUNDATION IN PEKALONGAN, CENTRAL JAVA. *International Journal of Remote Sensing and Earth Sciences (IJReSES)*, 10(2). <https://doi.org/10.30536/ijreses.2013.v10.a1845>



- Panchal, F. S., & Panchal, M. (2014). Review on Methods of Selecting Number of Hidden Nodes in Artificial Neural Network. *International Journal of Computer Science and Mobile Computing*, 3(11), 455–464.
- Pontoh, R. S., Toharudin, T., Ruchjana, B. N., Gumelar, F., Putri, F. A., Agisya, M. N., & Caraka, R. E. (2022). Jakarta Pandemic to Endemic Transition: Forecasting COVID-19 Using NNAR and LSTM. *Applied Sciences*, 12(12), 5771. <https://doi.org/10.3390/app12125771>
- Rayda, N. (2021, March 15). This city in Java could disappear in 15 years, due to land subsidence and coastal flooding. *Channel News Asia*. <https://www.channelnewsasia.com/climatechange/indonesia-pekalongan-land-sinking-coastal-flooding-disappear-1883156>
- Shahin, A. I., & Almotairi, S. (2021). A Deep Learning BiLSTM Encoding-Decoding Model for COVID-19 Pandemic Spread Forecasting. *Fractal and Fractional*, 5(4), 175. <https://doi.org/10.3390/fractalfract5040175>
- Siami-Namini, S., Tavakoli, N., & Namin, A. S. (2019). The Performance of LSTM and BiLSTM in Forecasting Time Series. *2019 IEEE International Conference on Big Data (Big Data)*, 3285–3292. <https://doi.org/10.1109/Big-Data47090.2019.9005997>
- Toharudin, T., Pontoh, R. S., Caraka, R. E., Zahroh, S., Lee, Y., & Chen, R. C. (2023). Employing long short-term memory and Facebook prophet model in air temperature forecasting. *Communications in Statistics - Simulation and Computation*, 52(2), 279–290. <https://doi.org/10.1080/03610918.2020.1854302>
- Vinata, R. T., Kumala, M. T., & Yustisia Serfiyani, C. (2023). Climate change and reconstruction of Indonesia's geographic basepoints: Reconfiguration of baselines and Indonesian Archipelagic Sea lanes. *Marine Policy*, 148, 105443. <https://doi.org/10.1016/j.marpol.2022.105443>
- Watson, R. T. (2001). *Climate Change 2001: Synthesis Report*.
- Yu, Z., Sun, Y., Zhang, J., Zhang, Y., & Liu, Z. (2023). Gated recurrent unit neural network (GRU) based on quantile regression (QR) predicts reservoir parameters through well logging data. *Frontiers in Earth Science*, 11. <https://doi.org/10.3389/feart.2023.1087385>
- Zahroh, S., Hidayat, Y., Pontoh, R. S., Santoso, A., & Talib Bon, A. (2019). Modeling and Forecasting Daily Temperature in Bandung Sukono. *Proceedings of the International Conference on Industrial Engineering and Operations Management Riyadh, Saudi Arabia*.
- Zhao, Z., Chen, W., Wu, X., Chen, P. C. Y., & Liu, J. (2017). LSTM network: a deep learning approach for short-term traffic forecast. *IET Intelligent Transport Systems*, 11(2), 68–75. <https://doi.org/10.1049/iet-its.2016.0208>



© 2024 by the authors; licensee Growing Science, Canada. This is an open access article distributed under the terms and conditions of the Creative Commons Attribution (CC-BY) license (<http://creativecommons.org/licenses/by/4.0/>).